

NONLINEAR DYNAMICS ANALYSIS OF A TWO-DEGREE-OF-FREEDOM DRY FRICTION VIBRO-IMPACT SYSTEM WITH SYMMETRIC CLEARANCES

Xingxiao CAO¹, Quanfu GAO²

The clearances and frictions among mechanical components exist widely in mechanical systems due to the demand for mechanical design and assembly errors. Clearances and frictions can cause vibration and noise, which have a great influence on performance of mechanical equipment. Studying the influence of clearances and frictions on system dynamics can optimize the mechanical system. A dynamic model of two-degree-of-freedom dry friction vibro-impact with symmetric clearances is established. The complicated dynamic behaviors are investigated by Runge-Kutta numerical method. The numerical simulation results indicate that the system exists complete 1-p-p fundamental periodic motions sequence. The chattering motion occurs when the impact number p is large enough. With decrease in frequency ω , the region of fundamental periodic motions becomes smaller, that of chaos becomes wider. The route of the fundamental periodic motion to chaos is similar, symmetric period motion transits into asymmetric period motion via pitchfork bifurcation, and finally falls into chaos via period-doubling bifurcation sequence. The mutual transition process between the fundamental periodic motions is complex and rich periodic motions overlapped each other, which is irreversible in some frequency range, thus a series of hysteresis zones occur, in which two types of periodic motions coexist.

Keywords: Clearance; Impact; Periodic motion; Bifurcation; Chaos

1. Introduction

In order to meet the needs of mechanical assembly, heat-expansion and cold-contraction, motion limiting constraints, the clearances or gaps exist in a wide variety of engineering applications between the primary components. Due to the clearance, the primary components will occur repeated impact and friction under external exciting force, as well as abrasion, noise and impact arise, which result in the accuracy and efficiency of the equipment decrease. Some severe cases may cause equipment damage and reduce service life. So the dynamics of the vibro-impact system with multi-degree-of-freedom and multi-clearance should

¹School of Mechanical Engineering, Lanzhou Jiaotong University, Lanzhou, China, e-mail: cxx2004@163.com

²School of Mechanical Engineering, Lanzhou Jiaotong University, Lanzhou, China, e-mail: gaoqf@mail.lzjtu.cn

be studied further, and it is very significant to the dynamics optimal design, reliability and noise controlling of mechanical system.

The scholars at home and abroad have done a lot of researches on vibro-impact and friction vibration system with clearances and constraints by qualitative analyses, numerical simulation and experiment. These studies involved dynamic stability [1-6], bifurcation [7-11], friction collision singularity [12-18], and chattering-impact vibration with sticking [19-23]. Nordmar [24] studied the singularity of Poincaré map caused by impact oscillator period orbits grazing rigid limit, found that with varying the control parameter, a special type of bifurcation, “grazing bifurcation” occurs in an impact oscillator and it was different from the conventional bifurcation of the continuous dynamical system, which laid a theoretical foundation for subsequent study of grazing bifurcation and singularity in this field. A two-degree-of freedom vibro-impact system with a rigid stop under periodic excitation was taken as the analysis object, diversity and evolution of periodic impact motions were analyzed in detail, and the correlative relationship and matching law between dynamic performance and key parameters are emphatically analyzed in Refs [25-26]. Budd and Dux [27] studied chattering impact motion and the role of chatter on vibro-impact dynamics. Wagg [28] numerically presented complete chattering and periodic sticking phenomena in a vibration system with two motion-limiting constraints and analyzed multi-sliding bifurcations of the system. Zhu and Luo [29] analyzed the dynamics characteristic of a two-degree-of freedom elastic vibro-impact system based on two-parameter and revealed the evolution law of the chattering-impact motion of the system. Virgin and Begley [30] studied global dynamics of the vibration impact system with Coulomb friction based on cell mapping method. They presented fully solution sets by studying the domain of attraction and found that bifurcation characteristic depended on the interactions of periodic attractor and domain of attraction, the grazing bifurcation caused catastrophic behaviors. Peterka [31] analyzed the influence of the dry friction on dynamic performances of the vibration impact system, and experimental study were carried. In view of the impact oscillator with dry friction, Cone and Zadoks [32] studied the pitchfork bifurcation, grazing bifurcation and stick-slip impact vibration, the existence of a subharmonic resonance motion that encompassed three periods of the forcing during each period was found. Ding et al. [33] studied the nonlinear dynamics of dry friction oscillator with symmetric clearance and found that pitchfork bifurcation existed in the system, the system became from symmetrical periodic motion to asymmetrical periodic motion, and then underwent Hopf bifurcation, period-doubling bifurcation and so forth to chaos.

There are many factors, such as impact, friction and time-varying stiffness, which cause the non-smooth or piece-wise smooth motion of the vibro-impact system for the practical mechanical system. The more the non-smooth factors are

considered, the more real the established dynamic model is. The previous research about the dynamic research on the non-smooth mechanical systems focused on single non-smooth factor, such as vibro-impact system, or vibration system with friction. Based on the related researches, this paper established a dry-friction/impact coupling dynamic model of the mechanical system and the effect of the dry friction on the dynamics of the vibro-impact system were investigated. The fundamental periodic motions sequence and route to chaos were studied, the transition irreversibility of adjacent impact motions with fundamental period and hysteresis were found. The formation of incomplete chattering motion of the system in low frequency was studied.

2. Mechanical model

The mechanical model of a two-degree-of-freedom dry friction oscillators with symmetric clearances is shown schematically in Fig. 1. The mass M_1 is connected to M_2 by a linear spring with stiffness K_1 and a viscous damper with damping constants C_1 , and mass M_2 is connected to rigid wall by a linear spring with stiffness K_2 and a viscous damper with damping constants C_2 . There is Coulomb friction between the two masses. There is an harmonic excitation force $P_i \sin(\Omega t + \tau)$ ($i=1, 2$) acting on the mass M_i . The static equilibrium position of the system is taken as the origin, and displacements of the masses M_1 and M_2 are expressed by X_1 and X_2 , respectively. There are symmetric clearances B between masses M_1 and M_2 . The mass M_1 impacts rigidly with the mass M_2 when the relative displacement $|X_1 - X_2| = B$.

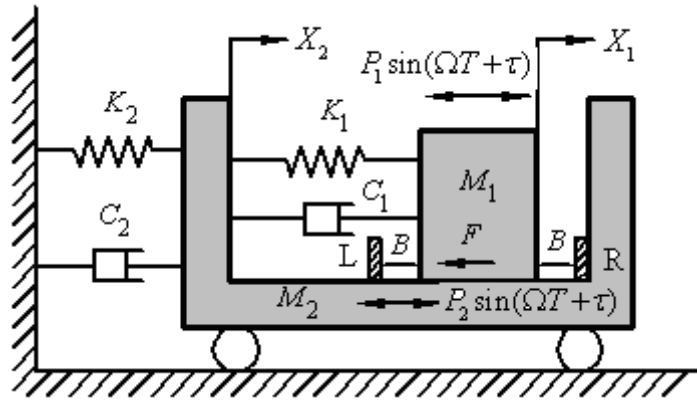


Fig. 1. The schematic of a two-degree-of-freedom vibro-impact system with symmetric clearances

In general, in order to study the dynamics of the vibro-impact system, some non-dimensional parameters should be introduced, and the values of system parameters can be determined easily if the dimensionless number is selected reasonably, which is important to study the parameter optimization and matching

law of the system. In the following work, we assume all parameters and variables are dimensionless, which are given by

$$\begin{aligned}\mu_m &= \frac{M_2}{M_1}, \mu_k = \frac{K_2}{K_1}, \mu_c = \frac{C_2}{C_1}, f_{20} = \frac{P_2}{P_1 + P_2}, f_k = \frac{F}{P_1 + P_2}, \omega = \Omega \sqrt{\frac{M_1}{K_1}}, t = T \sqrt{\frac{K_1}{M_1}}, \\ \zeta &= \frac{C_1}{2\sqrt{K_1 M_1}}, \quad b = \frac{B K_1}{P_1 + P_2}, \quad x_i = \frac{X_i}{P_1 + P_2} (i = 1, 2)\end{aligned}\quad (1)$$

Equation (1) allows us to make a conclusion that the sampling range of partial dimensionless parameters can be easily identified as $f_{20} \in [0, 1]$, where f_k denotes the sliding friction force between masses M_1 and M_2 .

Between the adjacent impacts, the system exist two states: slipping state and sticking state, due to the existing of friction F .

when, $|x_1 - x_2| < \delta$, $|\dot{x}_1 - \dot{x}_2| \neq 0$ the two masses are in slipping state, the non-dimensional equation is

$$\begin{aligned}\begin{bmatrix} 1 & 0 \\ 0 & \mu_m \end{bmatrix} \begin{bmatrix} \ddot{x}_1 \\ \ddot{x}_2 \end{bmatrix} + \begin{bmatrix} 2\zeta & -2\zeta \\ -2\zeta & 2\zeta(1 + \mu_c) \end{bmatrix} \begin{bmatrix} \dot{x}_1 \\ \dot{x}_2 \end{bmatrix} + \begin{bmatrix} 1 & -1 \\ -1 & 1 + \mu_k \end{bmatrix} \begin{bmatrix} x_1 \\ x_2 \end{bmatrix} \\ = \begin{cases} 1 - f_{20} \\ f_{20} \end{cases} \sin(\omega t + \tau) + \begin{bmatrix} -f_k \\ f_k \end{bmatrix} \operatorname{sgn}(\dot{x}_1 - \dot{x}_2) (|x_1 - x_2| < b)\end{aligned}\quad (2)$$

$$\text{where } \operatorname{sgn}(y) = \begin{cases} 1 & (y > 0) \\ 0 & (y = 0) \\ -1 & (y < 0) \end{cases} \quad (3)$$

Between the adjacent impacts, when $|\dot{x}_1 - \dot{x}_2| = 0$, the system may evolve into sticking state, when

$$\dot{x}_1 = \dot{x}_2, \quad \ddot{x}_1 = \ddot{x}_2 \quad (4)$$

thus the friction can be derived from equation (2) and (4) as follow

$$f_0 = \frac{\mu_m \sin(\omega t + \tau) + 2\zeta\mu_c \dot{x}_2 + \mu_k x_2 - (x_1 - x_2)}{1 + \mu_m} \quad (5)$$

When $|\dot{x}_1 - \dot{x}_2| = 0$ and $|f_0| \leq f_s$, the system evolves into sticking state, otherwise the mass M_1 continue sliding, just the direction of friction becomes opposite, where f_s is the maximum static friction of the system.

Under the sticking state, two masses stick together for synchronous motion and the system becomes forced vibration of single-degree-of-freedom oscillator with the mass $(M_1 + M_2)$, the non-dimensional equation becomes as follow:

$$\begin{cases} \ddot{x}_1 = \ddot{x}_2, \dot{x}_1 = \dot{x}_2 \\ (1 + \mu_m) \ddot{x}_2 + 2\zeta\mu_c \dot{x}_2 + \mu_k x_2 = \sin(\omega t + \tau) \end{cases} \quad (6)$$

During the sticking state, when $|f_0| > f_s$, the sticking state ends, the system evolves into sliding state again. And based on the f_0 , the sliding state exist in two states, namely $\dot{x}_1 - \dot{x}_2 > 0$ and $\dot{x}_1 - \dot{x}_2 < 0$, if $f_0 > 0$, then the system evolves into sliding state of the $\dot{x}_1 - \dot{x}_2 > 0$, otherwise, when $f_0 < 0$ the system evolves into sliding state of the $\dot{x}_1 - \dot{x}_2 < 0$.

Under the action of the friction, when the system is in sticking state, the impacts do not occur. During the sliding state, the impacts occur when $|x_1 - x_2| = b$, the impact equation becomes

$$\begin{cases} \dot{x}_{1-} + \mu_m \dot{x}_{2-} = \dot{x}_{1+} + \mu_m \dot{x}_{2+} \\ \dot{x}_{1+} - \dot{x}_{2+} = -R(\dot{x}_{1-} - \dot{x}_{2-}) \end{cases} \quad (7)$$

where, \dot{x}_{1-} and \dot{x}_{2-} denote the velocities of the mass M_1 and M_2 immediately before impact respectively, \dot{x}_{1+} and \dot{x}_{2+} denote the velocities of the mass M_1 and M_2 immediately after impact respectively.

The system illustrated in Fig. 1 may present multiple types of periodic motions under proper system parameters condition. In order to study the periodic motions visually, the symbol $n-p-q$ is introduced, where n ($n=1, 2, 3, \dots$) represents the cycle number of the excitations in an oscillation cycle, p and q ($p, q = 0, 1, 2, 3, \dots$) refer to the number of impacts of mass M_1 occurring on the left and right sides of the stop respectively, when $n=1$, $p=q$ ($p \geq 1$), which is called fundamental periodic motion particularly.

The system exhibits three motion states: sliding state, sticking state and impact state. Between the adjacent impacts, sliding state or sticking state occurs, sliding motion means two masses do not move in step, the sticking motion means the two mass move in step without impact. Under the sliding state, impact motion occurs once the $|x_1 - x_2| = \delta$, In general, the system may exhibit sliding state with the smaller friction coefficient and the sticking state will occur in the band of low frequencies with higher friction coefficient.

In order to identify which type of motion the system enters, we need to compute its time history by means of numerical computation. In general, the system for the sliding motion and the sticking motion, a fourth-order Runge-Kutta varying-step algorithm is used to solve the Eq. (2) and Eq. (6) with sufficient precision. However, it is difficult to confirm the point of transition from one pattern of motion to another. The accuracy of the conversion time is crucial to the accuracy of the results. Fixed-step $h_0=0.01$ is set initially in order to ensure that

all patterns of motions are contained, after every time step, the judgment of the motion pattern is made, once the motion pattern changes, the iteration will go back to the previous iterative point, and time step is decreased by one-tenth consecutively until the value of the transition time is precise to the order of 10^{-10} . The similar approach can be carried out for the value of the impact time. The numerical simulation program is written in C language in this paper.

Although the time history of the system can be determined with the above computational technique under any initial conditions, it hardly reveal any qualitative features of the system dynamics, which is conveniently studied by use of an impact Poincaré map derived from the equations of motion, supplemented by transition condition at the instant of impact. Here each iteration of this map corresponds to the point mass M_1 colliding with mass M_2 once at the constraint. The state of the vibro-impact system, just immediately after impact occurs at the constraint, is chosen as Poincaré section, i.e.,

$$\begin{aligned}\sigma_{qr} &= \{(x_1, \dot{x}_1, x_2, \dot{x}_2, \theta) \in R^4 \times S, x_1 - x_2 = b, \dot{x}_1 - \dot{x}_2 > 0\} \\ \sigma_{pl} &= \{(x_1, \dot{x}_1, x_2, \dot{x}_2, \theta) \in R^4 \times S, x_1 - x_2 = -b, \dot{x}_1 - \dot{x}_2 < 0\}\end{aligned}\quad (8)$$

3. Fundamental motions and route to chaos

The system with the non-dimensional parameters (1) $\mu_m = 10$, $\mu_k = 5$, $\mu_c = 5$, $\zeta = 0.1$, $b = 0.03$, $f_{20} = 0$, $f_s = 1.5f_k$, $R = 0.8$ and $\theta = \omega t$ are chosen as the standard parameter for analyses, the ω is taken as the control parameter.

The bifurcation diagrams for the system are shown in Fig. 2. Figs. 2(a)-(c) are the global bifurcation diagrams bifurcation diagrams for different frictions in the forcing frequency interval $\omega \in [1.0, 8.0]$. For $f_k = 0.01, 0.05$ and 0.1 , the frequency of pitch-fork bifurcation are $6.844, 6.81$ and 6.745 , which shows with the friction increases, the bifurcation frequency decrease in high frequency domain, but not very much. The region of the periodic motions becomes wider and that of chaos' becomes narrower in mid and low frequency domain, it is more obvious for low frequency, the system exhibits more periodic motions for the large f_k , which means the frictions have a greater impact on dynamics characteristics of the system in low frequency domain.

Figs. 2(d)-(f) are the local enlargement of the Fig. 2a. The simulative results show that with the decrease in ω , the system exists fundamental periodic motions sequence $1-1-1 \rightarrow 1-2-2 \rightarrow 1-3-3 \rightarrow \dots \rightarrow 1-p-p$. No sticking motion occurs due to the small friction, so the sticking and non-sticking motion are not marked.

With decrease in ω , the region of fundamental periodic motions becomes smaller, and the range of chaos becomes wider, the impact number p increases continuously and the impact velocity decreases continuously.

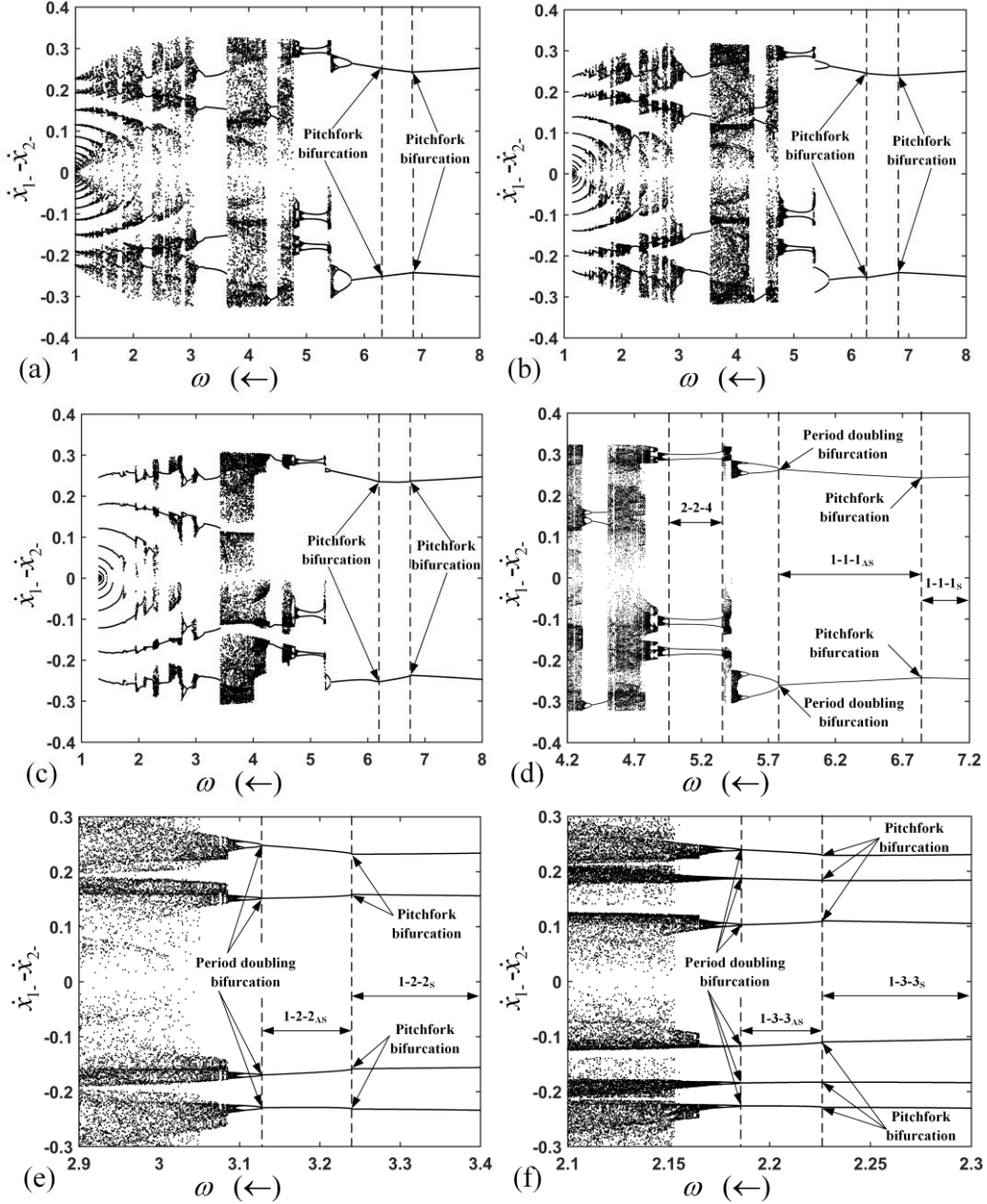


Fig. 2. The bifurcation diagram of (a) $f_k = 0.01$; (b) $f_k = 0.05$; (c) $f_k = 0.1$ (d)-(f) Local enlargements of (a): (d) $\omega \in [4.2, 7.2]$; (e) $\omega \in [2.9, 3.4]$; (f) $\omega \in [2.1, 2.3]$.

When the impact number p becomes large enough, the system occurs chattering motion. Chattering motion assumes different forms: incomplete and complete chattering, described by $1\tilde{p}\tilde{p}$ and $1\bar{p}\bar{p}$, respectively. The similarities of the two forms are that impact number p is sufficiently large during one forcing period ($n=1$), but for the former, the impact number p is finite, impact velocity do not reduce to zero and the two masses don't stick together at the rigid constraint. For the latter, the impact number p is infinite, impact velocity of the chattering sequence ultimately reduces to zero, which causes sticking motion of masses M_1 and M_2 at the rigid constraint.

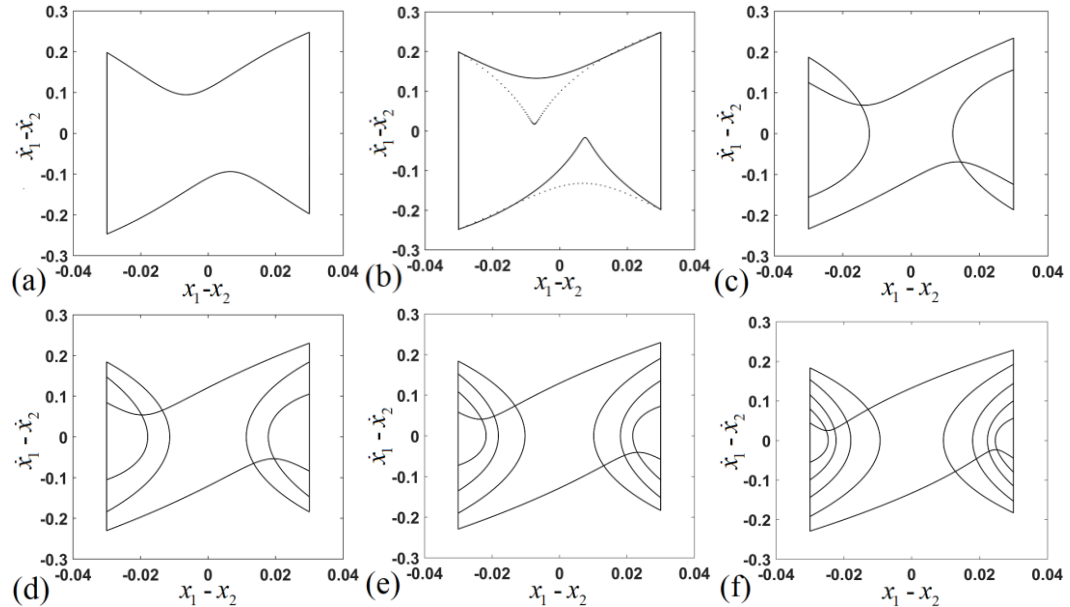


Fig. 3. Phase plane portraits of the fundamental periodic motion, $f_k = 0.01$

- (a) 1-1-1_S motion; $\omega = 7.5$; (b) 1-1-1_{AS} motion; $\omega = 6.5$; (c) 1-2-2_S motion, $\omega = 3.4$;
- (d) 1-3-3_S motion; $\omega = 2.3$; (e) 1-4-4_S motion; $\omega = 1.8$; (f) 1-5-5_S motion, $\omega = 1.5$.

The phase portraits of fundamental periodic motions sequence are shown in Fig. 3. The simulated results of the incomplete chattering motion are shown in Fig. 4 in the form of phase portraits, response diagram and projected Poincaré sections. There are two bifurcations, pitchfork bifurcation and period doubling bifurcation during the fundamental periodic motions 1-1-1 transits into chaos. The system exhibits single symmetric 1-1-1 fundamental periodic motion when $\omega > 6.844$. When ω passes through $\omega = 6.844$ decreasingly, pitchfork bifurcation occurs and symmetric 1-1-1_S fundamental periodic motion transits into asymmetric 1-1-1_{AS} fundamental periodic motion. The phase portraits of the symmetric and asymmetric 1-1-1 fundamental periodic motion are shown as Fig. 3a and Fig. 3b respectively. The asymmetric orbits, caused by different initial

conditions, is represented by dotted lines in Fig 3(b). With further decrease in the forcing frequency ω , finally the asymmetric 1-1-1_{AS} periodic motion transits into chaos via Feigenbaum period-doubling bifurcation sequence. The routes of the other fundamental periodic motion to chaos are similar to the 1-1-1 fundamental periodic motion.

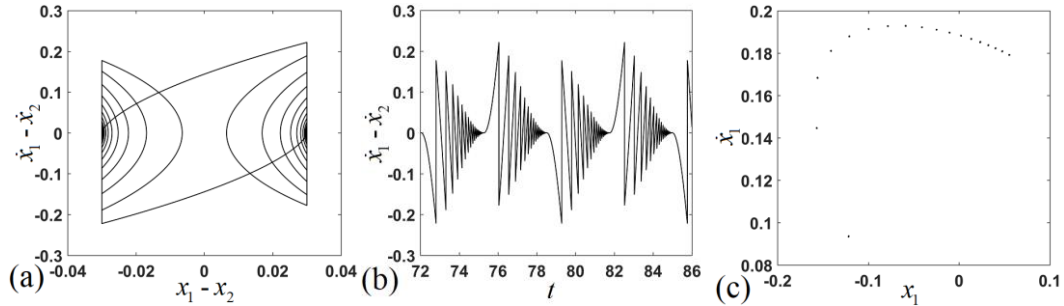


Fig. 4. Incomplete chattering 1-18-18 motion ($\omega=0.97$): (a) The phase plane portraits; (b) The time trajectories; (c) The Poincaré sections ($x_1 - x_2 = |b|$).

4. Mutual transition of the adjacent fundamental motions

Though the transition law of the fundamental periodic motion to chaos is similar, but chaos and complex periodic motions overlapped each other during the transition of the fundamental periodic motion. The mutual transition process is irreversible and complex phenomenon is more notable in the high frequency range. In order to investigate the transition law of the fundamental periodic motion, the transition zone between motion 1-1-1 and 1-2-2 is enlarged locally as Fig. 5. With decrease in ω , during the transition from fundamental periodic 1-1-1 motion to 1-2-2 motion, at first, 2-2-2 and 4-4-4 periodic motion via period doubling bifurcation occurs, and then the system falls into chaos via period doubling bifurcation sequences. With decrease in ω further, after a narrow window of chaos, 2-4-2 motion (maybe 2-2-4 motion occurs due to different initial conditions) is separated from the chaos via grazing bifurcation, as ω is decreased progressively, 2-4-2 motion undergoes a succession of period doubling bifurcation, which eventually results in chaotic motions, and the region of chaotic motion becomes wider than that of high forcing frequency. With decrease in ω further, 1-1-2 motion (maybe 1-2-1 motion occurs due to different initial conditions) is separated from the chaos, the system settles into chaotic motion again with ω decrease, finally, 1-2-2 symmetrical motion is generated after a wider region of chaos.

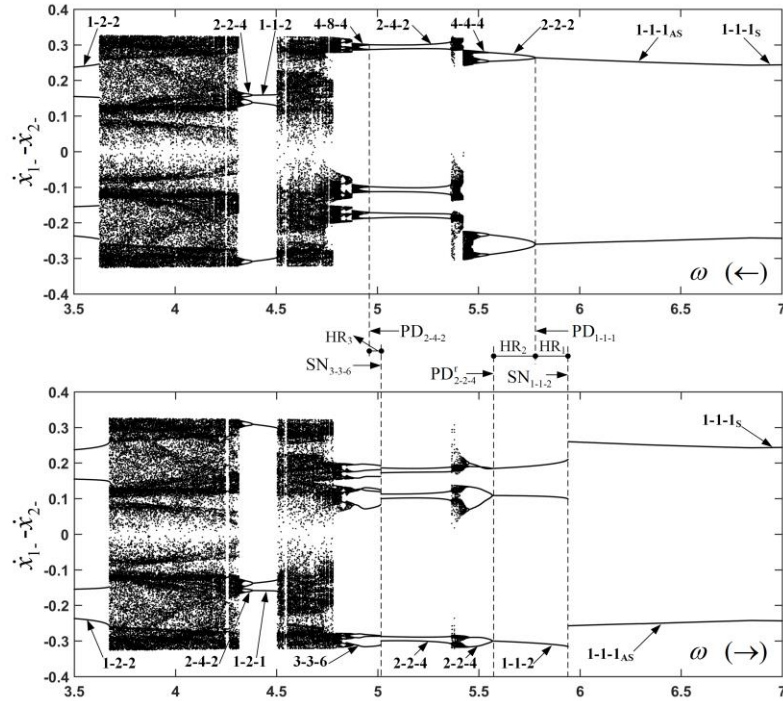


Fig. 5. The global bifurcation of $\omega - \dot{x}$, $f_k = 0.01$

In order to find mutual transition law of the adjacent fundamental periodic motions sequence, numerical analysis is carried out with the same system parameters and the same range of control parameter ω , the difference is that the control parameter ω changes from low to high as shown in Fig. 5. The transition law is similar in the forcing frequency interval $\omega \in [3.5, 4.8]$, but it is markedly different in the forcing frequency interval $\omega \in [4.8, 5.942]$ compared with that ω decrease. When the ω decreases in the region, the bifurcations are period doubling bifurcations, but when the ω increases in the same region, at first, 3-3-6 motion is separated from the chaos via reverse period doubling bifurcation, and then 2-2-4 motion occurs via Saddle-node bifurcation, we can observe that the value of ω increase of the bifurcation occurs is different when the ω varies in different direction as shown in Fig. 5.

As shown in Fig. 5, there three hysteresis intervals in the transition zone between motion 1-1-1 and 1-2-2, two types of periodic motions are stable and can coexist depending on the initial conditions of the system in the hysteresis intervals, we name it hysteresis zone, denoted with HR. The bifurcation boundary of HR is marked with dotted lines. Here, SN_{n-p-q} , PD_{n-p-q} and PD_{n-p-q}^r denote the curves of Saddle-node, period doubling bifurcation and reverse period doubling bifurcation of $n-p-q$ motion, respectively. The first hysteresis zone HR_1 is formed

by two curves SN_{1-1-2} ($\omega = 5.942$) and PD_{1-1-1} ($\omega = 5.79$), in which the 1-1-2 motion and 1-1-1_{AS} motion coexist, the phase portrait of this periodic motion is shown in Fig. 6(a) and 6(d). The second hysteresis zone HR_2 is formed by two curves PD_{1-1-1} ($\omega = 5.79$) and PD_{2-2-4}^r ($\omega = 5.575$), in which 1-1-2 motion and 2-2-2_{AS} motion coexist, the phase portrait of this periodic motion is shown in Fig. 6(b) and 6(e), the third hysteresis zone HR_3 is formed by two curves SN_{3-3-6} ($\omega = 5.015$) and PD_{2-4-2} ($\omega = 4.962$), where 2-4-2 motion and 3-3-6 motion coexist, the phase portrait of this periodic motion is shown in Fig. 6(c) and 6(f).

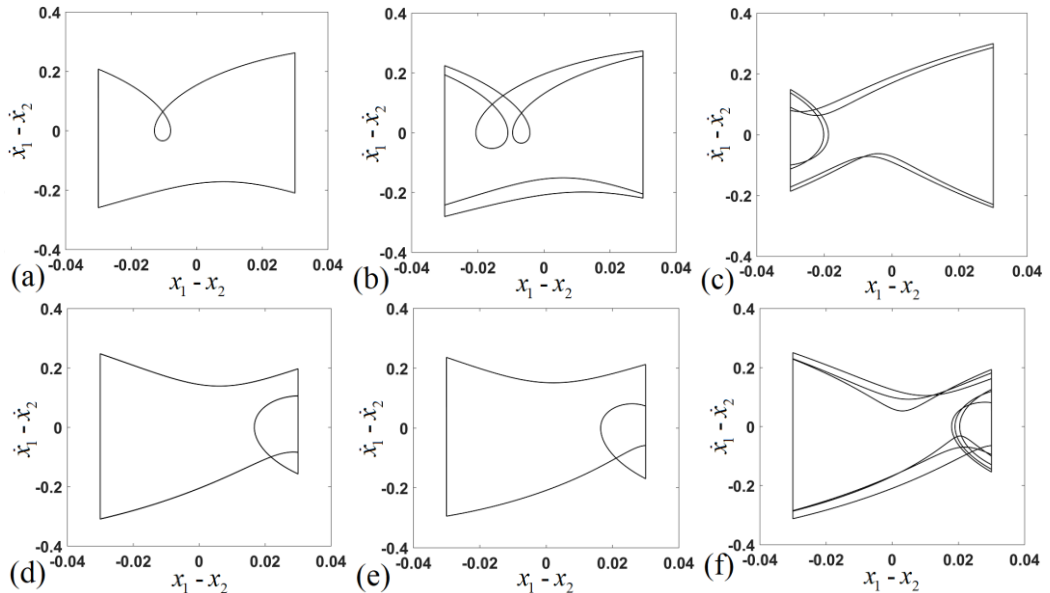


Fig. 6. Phase plane portraits of the hysteresis zone:
 (a) $\omega = 5.85$, 1-1-1_{AS} motion; (b) $\omega = 5.67$, 2-2-2_{AS} motion; (c) $\omega = 5.01$, 2-4-2 motion;
 (d) $\omega = 5.85$, 1-1-2 motion; (e) $\omega = 5.67$, 1-1-2 motion; (f) $\omega = 5.01$, 3-3-6 motion.

5. Conclusions

Dynamics analysis of a two-degree-of-freedom dry friction vibro-impact system with symmetric clearances are studied. The judgment method of the sticking motion and sliding motion of the system are given. Complicated dynamics analysis are carried out by numerical simulation. Numerical simulation results indicate that the system exist complete 1- p - p fundamental periodic motions sequence. With decrease in ω , the region of fundamental periodic motions becomes smaller, and the region of chaos becomes wider. The impact number p increases continuously and the impact velocity decreases continuously with

decrease in ω , when the impact number p becomes large enough, the system occurs chattering motion.

The route of the fundamental periodic motion to chaos is similar, i. e., with decrease in ω , symmetric 1-1-1 fundamental periodic motion transits into asymmetric 1-1-1AS fundamental periodic motion via pitchfork bifurcation, and finally falls into chaos via period-doubling bifurcation sequence.

The mutual transition process between the adjacent fundamental 1- p - p periodic motions is complex and rich periodic motions overlapped each other when the ω in high frequency, which is irreversible in some frequency range. Reverse period doubling bifurcation and Saddle-node bifurcation occur when ω sweeps in increasing direction, but period doubling bifurcation occurs when ω sweeps in decreasing direction. Due to the value of the bifurcation parameter is different, thus a series of hysteresis zone occurs in which two types of periodic motions coexist.

6. Acknowledgement

This work was supported by the Natural Science Foundation of Gansu Province, China (18JR3RA118), the Project of Lanzhou Science and Technology Bureau (2015-3-106) and Foundation of A Hundred Youth Talents Training Program of Lanzhou Jiaotong University.

R E F E R E N C E S

- [1]. S. W. Shaw, P. J. Holmes. “A periodically forced piecewise linear oscillator”, Journal of Sound and Vibration, **vol. 90**, no. 1, 1983, pp. 129-155.
- [2]. F. Peterka, J. Vacik. “Transition to chaotic motion in mechanical systems with impacts”, Journal of Sound and Vibration, **vol. 154**, no. 1, 1992, pp. 95-115.
- [3]. J. O. Aidanpää, R. B. Gupta. “Periodic and chaotic behaviour of a threshold-limited two-degree-of-freedom system”, Journal of Sound and Vibration, **vol. 165**, no. 2, 1993, pp. 305-327.
- [4]. J. Knudsen, A. R. Massih. “Dynamic stability of weakly damped oscillators with elastic impacts and wear”, Journal of Sound and Vibration, **vol. 263**, no. 1, 2003, pp. 175-204.
- [5]. QH. Li, QS. Lu, “Coexisting periodic orbits in vibro-impacting dynamical systems”, Applied Mathematics and Mechanics, **vol. 24**, no. 3, 2003, pp. 261-273.
- [6]. R. I. Leine. “Non-smooth stability analysis of the parametrically excited impact oscillator”, International Journal of Non-Linear Mechanics, **vol. 47**, no. 9, 2012, pp. 1020-1032.
- [7]. K. Czolczynski, A. Okolewski, B. Blazejczyk-Okolewska. “Lyapunov exponents in discrete modelling of a cantilever beam impacting on a moving base”, International Journal of Non-Linear Mechanics, **vol. 88**, 2017, pp. 74 -84.
- [8]. J. H. Xie, W. C. Ding, E. H. Dowell, L. N. Virgin. “Hopf-flip bifurcation of high dimensional maps and application to vibro-impact systems”, Acta Mechanica Sinica, **vol. 21**, no. 4, 2005, pp. 402-410.

- [9]. *Y. Yue*, “Local dynamical behavior of two-parameter family near the Neimark-Sacker-pitchfork bifurcation point in a vibro-impact system”, Chinese Journal of Theoretical and Applied Mechanics, **vol. 48**, no. 1, 2016, pp. 163-172.
- [10]. *Y. Zhang, G. W. Luo*. “Detecting unstable periodic orbits and unstable quasiperiodic orbits in vibro-impact systems”, International Journal of Non-Linear Mechanics, **vol. 96**, 2017, pp. 12-21.
- [11]. *F. Guo, J. X. Pan, Y. Mu, Z. D. Jin*. “The dynamic property and chaos control for a two-degree-of-freedom vibro-impact system”, UPB Scientific Bulletin, Series D: Mechanical Engineering, **vol. 180**, no. 1, 2018, pp. 29-42.
- [12]. *H. B. Jiang, A. S. E. Chong, Y. Ueda, M. Wiercigroch*. “Grazing-induced bifurcations in impact oscillators with elastic and rigid constraints”, International Journal of Mechanical Sciences, **vol. 127**, 2017, pp. 204-214.
- [13]. *H. Y. Hu*. “Detection of grazing orbits and incident bifurcations of a forced continuous, piecewise-linear oscillator”, Journal of Sound and Vibration, **vol. 187**, no. 3, 1995, pp. 485-493.
- [14]. *A. P. Ivanov*. “Stabilization of an impact oscillator near grazing incidence owing to resonance”, Journal of Sound and Vibration, **vol. 162**, 1993, no. 3, pp. 562-565.
- [15]. *S. Kryzhevich, M. Wiercigroch*. “Topology of vibro-impact systems in the neighborhood of grazing”, Physica D, **vol. 241**, no. 22, 2012, pp. 1919-1931.
- [16]. *Y. G. Huangfu, Q. H. Li*, “Grazing bifurcation of a vibrating cantilever system with on-sided impact”, Chinese Journal of Theoretical and Applied Mechanics, **vol. 40**, no. 6, 2008, pp. 812-819.
- [17]. *N. Humphries, P. T. Piiroinen*. “A discontinuity-geometry view of the relationship between saddle-node and grazing bifurcations”, Physica D, **vol. 241**, no. 22, 2012, pp. 1911-1918.
- [18]. *J. Feng, W. Xu*, “Grazing-induced chaotic crisis for periodic orbits in vibro-impact systems”, Chinese Journal of Theoretical and Applied Mechanics, **vol. 45**, no. 1, 2013, pp. 30-36.
- [19]. *C. Toulemonde, C. Gontier*. “Sticking motions of impact oscillators”, European Journal of Mechanics. A: Solids, **vol. 17**, no. 2, 1998, pp. 339-366.
- [20]. *S. Ema, E. Marui*. “Suppression of chatter vibration of boring tools using impact dampers”, International Journal of Machine Tools and Manufacture, **vol. 40**, no. 8, 2000, pp. 1141-1156.
- [21]. *A. B. Nordmark, P. T. Piiroinen*. “Simulation and stability analysis of impacting systems with complete chattering”, Nonlinear Dynamics, **vol. 58**, no. 1-2, 2009, pp. 85-106.
- [22]. *Albert C. J. Luo, Dennis O'Connor*. “Mechanism of impacting chatter with stick in a gear transmission system”, International Journal of Bifurcation and Chaos, **vol. 19**, no. 6, 2009, pp. 2093-2105.
- [23]. *Csaba Hős, Alan R. Champneys*, “Grazing bifurcations and chatter in a pressure relief valve model”, Physica D, **vol. 241**, no. 22, 2012, pp. 2068-2076.
- [24]. *A. B. Nordmark*. “Non-periodic motion caused by grazing incidence in an impact oscillator”, Journal of Sound and Vibration, **vol. 145**, no. 2, 1991, pp. 279-297.
- [25]. *G. W. Luo, X. H. Lv, Y. Q. Shi*. “Vibro-impact dynamics of a two-degree-of freedom periodically-forced system with a clearance: Diversity and parameter matching of periodic-impact motions”, International Journal of Non-Linear Mechanics, **vol. 65**, 2014, pp. 173-195.
- [26]. *G. W. Luo, X. F. Zhu, Y. Q. Shi*. “Dynamics of a two-degree-of freedom periodically-forced system with a rigid stop: Diversity and evolution of periodic-impact motions”, Journal of Sound and Vibration, **vol. 334**, 2015, pp. 338-362.

- [27]. *C. Budd, F. Dux*. “Chattering and related behaviour in impact oscillators”, *Philos Trans, Roy Soc A*, **vol. 347**, no. 1683, 1994, pp. 365-389.
- [28]. *D. J. Wagg*. “Multiple non-smooth events in multi-degree-of-freedom vibro-impact systems”, *Nonlinear Dynamics*, **vol. 43**, 2006, pp. 137-148.
- [29]. *X. F. Zhu, G. W. Luo*, “Chattering-impact motion of a 2-DOF system with clearance and soft impacts”, *Journal of Vibration and Shock*, **vol. 34**, no. 15, 2015, pp. 195-200.
- [30]. *L. N. Virgin, C. J. Begley*, “Grazing Bifurcation and Basins of Attraction in an Impact-friction Oscillator”, *Physica D*, **vol. 130**, no. 1-2, 1999, pp. 43-57
- [31]. *F. Peterka*. “Analysis of Motion of the Impact-dry-friction pair of Bodies and its Application to the Investigation of the Impact Dampers Dynamics”, *Proceedings of the ASME Design Technical Conference*, Las-Vegas: ASME, 1999, pp. 12-15.
- [32]. *K. M. Cone, R. I. Zadoks*, “A numerical study of an impact oscillator with the addition of dry friction”, *Journal of Sound and Vibration*, **vol. 188**, no. 5, 1995, pp. 659-683.
- [33]. *W. C. Ding, Y. X. Zhang, J. H. Xie*, “Analysis of Nonlinear Dynamics of Dry Friction Oscillators with Symmetric Clearance”, *Tribology*, **vol. 28**, no. 2, 2008, pp. 155-160.